J. Fluid Mech. (1996), *vol.* 317, *pp.* 73–90

Hydrodynamics of scallop locomotion: unsteady fluid forces on clapping shells

By J.-Y. CHENG AND M. E. DEMONT
Department of Biology, St Francis Xavier University, PO Box 5000, Antigonish, Nova Scotia, B2G 2W5, Canada

(Received 1 March 1995 and in revised form 9 November 1995)

A potential flow model has been formulated for scallop swimming. Under the small-disturbance approximation, the problem of the unsteady flow past the wing-like configuration of a scallop is separated into two linear sub-problems: the steady lifting problem and the unsteady symmetric thickness problem. The latter is associated with the expansion and contraction of the boundary surface of the scallop due to the shell opening and closing. A quasi-two-dimensional analytical solution of the thickness problem was obtained to give the time-dependent fluid forces acting on the outer surfaces of the shells. In addition to the added-mass effect, which has been widely accepted in the hydrodynamics of aquatic locomotion, there are two other mechanisms in the fluid reaction: flow-induced pseudo-elasticity and pseudo-viscosity. The pseudo-elasticity provides a force proportional to the gape angle displacement, and will assist shell opening but resist shell closing. The pseudo-viscosity force is proportional to the angular velocity of the gape, and benefits both shell opening and closing. Their roles are discussed through comparison with those of shell inertia, hinge ligament elasticity and hinge damping. At 10 °C the hinge damping in the scallop was found to be almost compensated by the flow pseudo-viscosity. The unsteady fluid reaction may have a significant effect on the operation of the dynamic swimming system of scallops.

1. Introduction

Scallops are one of the few bivalve mollusca that have evolved the ability to swim, and use this ability to avoid natural predators, and to seasonally migrate. The mechanics and hydrodynamics of scallop swimming have received the attention of many researchers. Jet propulsion has been studied for scallops (Moore & Trueman 1971; Gould 1971) and other aquatic animals (Trueman 1975; Alexander 1977; Weihs 1977; O'Dor 1988; DeMont & Gosline 1988; Madin 1990). Stanley (1970) and Gould (1971) emphasized the importance of hydrodynamic lift in overcoming gravity. Some hydrodynamic characteristics were measured for several species (Gould 1971; Morton 1980; Dadswell & Weihs 1990) to understand the observations that some species swim better than others and to examine scale effects of swimming ability. Gruffydd (1976) measured the hydrodynamic lift on scallops in current. Hayami (1991) and Millward & Whyte (1992) experimentally studied the lift and drag on living and fossil scallop shells.

Scallops, as bivalves, consist of two shells (valves) that are held together by an elastic hinge (figures 1 and 2). The shells can be rapidly pulled together by the contraction of a single adductor muscle, which is the part of the animal consumed by people. The water is expelled out of the cavity between the shells (mantle cavity) during the shell closing. The animal then keeps its shells closed to glide for a while. Strain energy stored in the ligaments during shell closure is released as the muscle relaxes to open the shells,

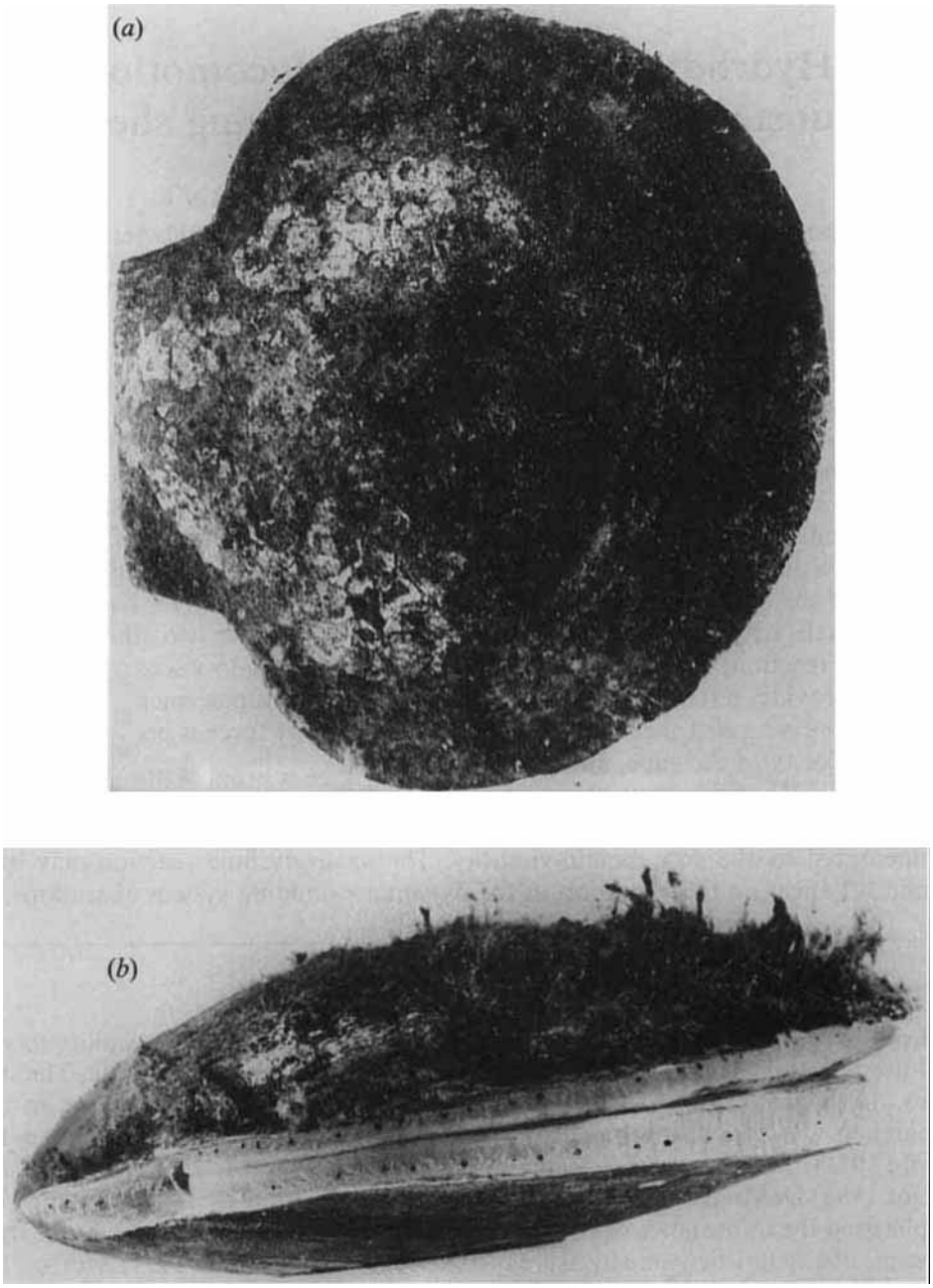

FIGURE 1. A photograph of a scallop, *Placopecten magellanicus*, with a shell height (S_L) of 0.13 m: (*a*) top view; (*b*) side (posterior) view. The photograph was taken with the animal resting on the substrate. The ventral anterior shell is covered with various algae and invertebrates. In the posterior view, the shells are gaped for feeding, and the velum contains many ocelli (black dots) that form the 'eyes'.

meanwhile the water is drawn into the cavity under the regulation of the velum between the two shells. After reaching the maximum shell opening the velum is sealed and the adductor muscle is activated to close the shells again.

Scallops swim with the ventral region foremost and are propelled by pulsed jets

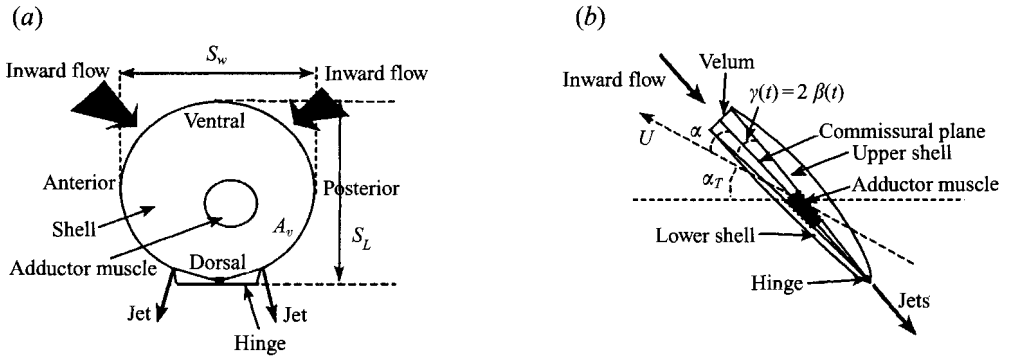

FIGURE 2. Schematic diagrams of a scallop corresponding to those shown in figure 1: (*a*) top view when the upper shell is removed, A_v is the valve area, S_w shell width, S_L shell height; (*b*) side (anterior) view, α is the angle of attack, α_T the trajectory angle between the swimming direction and horizontal surface. The gape angle $\gamma(t) = 2\beta(t)$ is used to describe the shells opening and closing around the hinge.

(figure 2). Level swimming is achieved by periodic propulsive jets directed backward from two orifices near the dorsal hinge. Generally, one sustained bout of swimming may last several seconds and the distance covered can be hundreds of centimetres. One scallop of the species *Amusium pleuronectes*, was recorded to swim for 18 s, covering a distance of 10 m in a laboratory condition (Morton 1980). The typical mean swimming speed is about 0.45 m s^{-1} for *Placopecten* (Dadswell & Weihs 1990). A maximum swimming speed of 0.73 m s^{-1} was found for a 0.07 m *Amusium* (Morton 1980). Dadswell & Weihs (1990) reported a maximum speed of 0.79 m s^{-1} for a 0.06 m *Placopecten*.

The sea scallop *Placopecten magellanicus* (figure 1) is one of the most important species of molluscan shellfish that is commercially fished in Canada. The scallops are captured by nets (drags) that are pulled along the ocean floor. The ability of the animals to see the drag approaching and to escape capture has initiated an extensive study to predict swimming ability under various environmental conditions. The body length of these animals (shell height) reaches a maximum of about 0.15 m. For a 0.065 m long *Placopecten*, the clapping period is around 0.3 s, during which about 0.017 kg of sea water is sucked into the mantle cavity and then expelled out.

The external fluid forces acting on each of the two shells during swimming is time-dependent and associated with shell opening and closing. The pressure difference between the upper and lower shells contributes to the net lifting force and induced drag. The instantaneous force on the external surface of each shell will affect the valve opening and closing and thus the dynamics of the locomotor system, consisting of the muscle, the dorsal hinge ligaments and the shells. Vogel (1985) measured the importance of flow in assisting shell reopening, but only steady flows were considered. The unsteady fluid reaction on each shell, which has not been measured yet, must be evaluated in order to quantify the energetics of locomotion in scallops (DeMont 1990; Marsh, Olson & Quzik 1992; Bowie, Layes & DeMont 1993). Such an unsteady hydrodynamic force acting on the external surface of the animal has been omitted in many previous studies on the energetics of jet-propelled aquatic locomotion.

The potential flow theory for low-speed aerodynamics may be used to study scallop swimming in water, since scallops have a wing-like configuration and the outer flow around the shells is associated with large Reynolds numbers. Assuming small disturbances, the problem of unsteady flow past a thin wing can be separated into two

linear sub-problems, namely the asymmetric lifting and symmetric thickness problems. The thickness problem is always unsteady, even for steady swimming, and provides the fluid force which interacts with the force generated by the contraction of the adductor muscle. During a shell clapping cycle, the thickness increases when the shells open and decreases when the shells close. The unsteady lifting surface has been extensively studied in unsteady aerodynamics with particular application to aeroelasticity, stability and stall (Belotserkovskii 1977; McCroskey 1982), and also to fish swimming (Lighthill 1975; Ahmadi & Widnall 1986; Blickhan & Cheng 1994). The unsteady thickness problem was generally considered to have no practical meaning and has received little consideration in conventional unsteady aerodynamics. Scallop swimming provides a biological example that shows the importance of the unsteady thickness effect.

In this paper we will formulate the unsteady potential flow problem resulting from scallop swimming. A quasi-two-dimensional analytical solution is derived for the unsteady thickness problem. The unsteady fluid force and moment about the hinge acting on the external surface of each shell are obtained. The properties of the force and moment are discussed to demonstrate the possible effect on the dynamic swimming system. This result has been combined with the mechanical properties of the hinge (DeMont 1990; Bowie *et al.* 1993), the measured kinematics and internal fluid pressure to study the dynamics and energetics of scallop swimming, and to predict the *in vivo* muscle performance (Cheng, Davison & DeMont 1996).

2. Fluid-dynamic model

2.1. *Formulation of potential flow model*

Scallops are assumed to swim at a speed $U(t)$ in an otherwise undisturbed fluid. An instantaneous body coordinate system (x, y, z) is attached to the scallop with the (x, y)-plane coinciding with the average plane of the upper and lower shells (the commissural plane). The x-axis crosses the hinge axis at a right angle. In this body system, the oncoming flow of velocity $U(t)$ has an angle of attack with the x-axis, $\alpha(t)$. The shells open and close in the z-direction. Level swimming is considered so that the trajectory angle is zero (figure 3).

If we do not consider the flow between the valves, scallop swimming is associated with large Reynolds number, close to or larger than 10^4 for *Placopecten magellanicus* (Dadswell & Weihs 1990). The viscous effect is important only in the thin boundary layer in which the friction drag can be determined. The fluid flow outside the boundary layer and wake can be considered as an irrotational inviscid incompressible flow, i.e. potential flow.

For potential flow, a velocity potential $\Phi(x, y, z, t)$ exists and is governed by the Laplace equation

$$\Delta\Phi(x, y, z, t) = 0. \tag{1}$$

The velocity field is

$$\boldsymbol{V}(x, y, z, t) = \nabla\Phi. \tag{2}$$

Since the disturbance induced by the movement of the scallop will decay far from the body, in the body system we have

$$\lim_{r\to\infty} \boldsymbol{V} = U(t)(\cos\alpha\boldsymbol{i} + \sin\alpha\boldsymbol{j}). \tag{3}$$

The outer boundary of the scallop at any instant can be written as

$$B(x, y, z, t) = z - h(x, y, z, t) = 0. \tag{4}$$

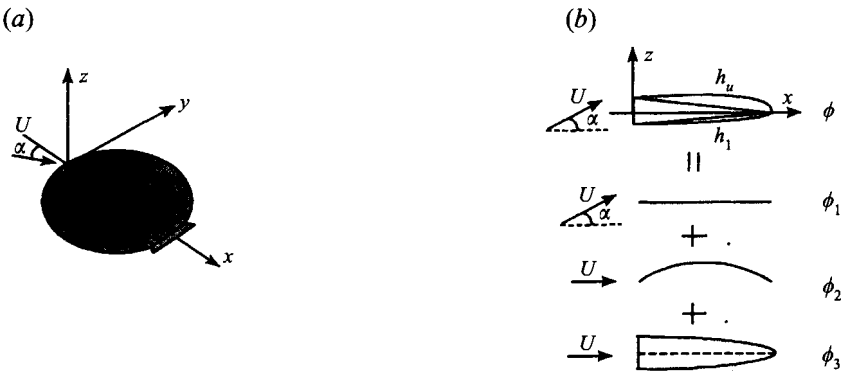

FIGURE 3. (*a*) Coordinate system for a swimming scallop. (*b*) Decomposition of the problem of the changing thickness, cambered scallop swimming at an angle of attack into three sub-problems.

The no-penetration condition on the solid surface requires that the normal component of the relative velocity on the solid boundaries must be zero. There is an outward flow (propulsive jets) from the orifices in the dorsal direction during shell closing, and an inward flow sucked into the cavity through the ventral mantle margin that is regulated by the velum during shell opening. The instantaneous volume of the expellable water enclosed by the velum and the two shells is determined by the position of the two shells. According to the principle of conservation of mass, during any time interval the expelled water equals the reduction of water mass in the cavity. Thus the velocity of the jet, U_j, is a function of the shell clapping velocity and the geometries of the cavity and jets. In principle, the velocity of the inward flow, U_i, can be similarly determined. Hence we have the boundary condition on the scallop surface as

$$(\nabla\Phi - V_r)|_{B=0} \cdot \boldsymbol{n} = \begin{cases} 0 & \text{on shells} \\ U_j & \text{on jet orifices, } t \in \Delta t_c, \\ U_i & \text{on velum, } t \in \Delta t_o, \end{cases} \tag{5}$$

where $\boldsymbol{n}(x, y, z, t)$ is the outward normal to the surface of the scallop, $V_r(x, y, z, t)$ the relative velocity of the surface due to the clapping of the shells in the body system and determined by (3), Δt_c ad Δt_o are the time intervals of the shell closing and opening, respectively. Thus the potential flow around a swimming scallop is determined by equations (1)–(5) and the Kutta condition, which requires zero loading at the trailing (dorsal hinge axis) edge. Once the velocity potential is obtained, the corresponding pressure field can be calculated from Bernoulli's equation.

2.2. *Flow around a sealed body and the small-disturbance approximation*

The problem presented above will be simplified in this section. The jet opening is very small, and the mean cross-sectional area is about 1% or less of the shell area (our measurements). The time duration of the shell closing phase is about one third of one clapping period. The jet flow from the hinge orifice during shell closing is assumed to have no influence on the flow around the body. The water is drawn into the cavity through the mantle margin along most of the periphery of the shells. The detailed processes of the flow sucking into the cavity during shell opening have not been observed. The inward flow may reduce the fluid pressure near the ventral opening and

subsequently the magnitude of the perturbation velocity of the flow around the animal. However, it is likely that the cavity is filled instantly while the shells are opening, since the animal is immersed in the infinite fluid medium and the shell opening is towards the swimming direction. The shell opening phase also only occupies about one third of one clapping period. Although the inward flow may affect the flow around the body during shell opening, the difference between the external flow around the swimming scallop with and without the inward flow is not expected to be significant. The inward flow will be ignored here.

In the body system, the total velocity potential is composed of the potential due to the oncoming flow and the perturbation potential induced by the animal, i.e.

$$\Phi(x,y,z,t) = \Phi_o(x,y,z,t) + \phi(x,y,z,t) = U(t)(x\cos\alpha + z\sin\alpha) + \phi(x,y,z,t), \quad (6)$$

where the perturbation potential $\phi(x,y,z,t)$ is also governed by the Laplace equation. From (3) and (6), the boundary condition at infinity for the perturbation potential ϕ now becomes

$$\lim_{r\to\infty} \nabla\phi = 0. \quad (7)$$

Substituting (4) and (6) into the no-penetration condition (5) on the shells, we have

$$\frac{\partial\phi}{\partial z} = \left(U\cos\alpha + \frac{\partial\phi}{\partial x}\right)\frac{\partial h}{\partial x} + \frac{\partial\phi}{\partial y}\frac{\partial h}{\partial y} - U\sin\alpha + \frac{\partial h}{\partial t}, \quad \text{on shells.} \quad (8)$$

For steady swimming, we assume that the scallop swims at a constant speed U which may be obtained by averaging the instantaneous swimming speed over several clapping cycles. There have been no detailed kinematic studies of the instantaneous swimming speeds of scallops. However, our observations indicate that a constant speed swimming can be a good approximation to real swimming. The instantaneous thickness of the scallop is the sum of the steady position when the shell is closed and the increment due to the shell opening. The maximum thickness is located a little behind the centre of the shell. The ratio of the maximum thickness of scallops when the shells are closed to the shell height ranges from about 0.2 to 0.3 for most species (Dadswell & Weihs 1990; Millward & Whyte 1992). The increment in the thickness due to the shell opening increases from zero at the hinge to the maximum at the ventral tip. The ratio of the increased thickness due to the shell opening to the shell height is about 0.157 at the ventral tip when gaped at the mean value of 9° for *Placopecten magellanicus* (Dadswell & Weihs 1990). Thus the maximum total thickness ratio is about 0.28 to 0.38. On average, the thickness ratio changes from 0.25 to 0.33 during a clapping cycle of regular swimming for most species. Furthermore, the mean angle of attack of level swimming is small and about 6° for *Placopecten magellanicus* (Dadswell & Weihs 1990). Thus it seems reasonable that the classical small-disturbance approximation can be used to obtain the first-order perturbation solution for the problem of the swimming scallop.

If we assume the velocity perturbations caused by the motion of the scallop to be small, i.e.

$$\left|\frac{\partial\phi}{\partial x}\right|, \left|\frac{\partial\phi}{\partial y}\right|, \left|\frac{\partial\phi}{\partial z}\right| \ll U \quad (9)$$

and keep all terms of first-order small quantities, (7) becomes

$$\frac{\partial\phi(x,y,0,t)}{\partial z} = U\left(\frac{\partial h}{\partial x} - \alpha\right) + \frac{\partial h}{\partial t}, \quad (x,y\in A_v), \quad (10)$$

where A_v is the average projected domain of the shells on the (x, y)-plane (commissural plane). This is a linear boundary condition which has been transferred to the $z = 0$ plane.

The velum (pallial curtain) between the parted valves regulates the flow through the ventral mantle margin. When the shells are not closed, the outer surface of the velum can be viewed approximately as part of a cylindrical boundary with its longitudinal axis in the z-direction. Thus the external surface of the sealed body is composed of the upper and lower shells and the wall of the cylinder segment cut by the shells.

The swimming movement is achieved by the clapping of two rigid shells. The shell oscillation may be described by the time-dependent gape angle, $\gamma(t)$ (figure 2*b*). During free swimming, either shell can be viewed at any time as opening by half of the gape angle with respect to the commissural plane, i.e. $\beta(t) = \frac{1}{2}\gamma(t)$. The instantaneous position of the outer surfaces of the upper and lower solid shells in the body coordinate system may be described by

$$z = h(x, y, t) = \begin{cases} h_p(x, y, t) = h_{ps}(x, y) + h_{pu}(x, t) = h_{ps} + \beta(t)(S_L - x), & z > 0 \\ h_w(x, y, t) = h_{ws}(x, y) + h_{wu}(x, t) = h_{ws} - \beta(t)(S_L - x), & z < 0 \end{cases} \quad (x, y \in A_v), \tag{11}$$

where S_L is the body length (shell height), the subscripts p and w represent the upper and lower shells, s and u represent the steady and unsteady quantities, $h_{ps}(x, y)$ and $h_{ws}(x, y)$ are the steady parts of the position of the upper and lower shells when the shells are closed, and $h_{pu}(x, y)$ and $h_{wu}(x, y)$ are the unsteady parts of the shell position due to the shell clapping. Defining a camber function h_c and a thickness function h_t as

$$\left.\begin{aligned} h_c(x, y, t) &= \tfrac{1}{2}(h_p + h_w) = \tfrac{1}{2}(h_{ps} + h_{ws}) = h_{cs}(x, y), \\ h_t(x, y, t) &= \tfrac{1}{2}(h_p - h_w) = \tfrac{1}{2}(h_{ps} - h_{ws}) + \beta(t)(S_L - x) = h_{ts}(x, y) + h_{tu}(x, t), \end{aligned}\right\} \tag{12}$$

then the upper and lower shell surfaces of the scallop in (11) can be expressed as

$$h_p = h_c + h_t, \quad h_w = h_c - h_t. \tag{13}$$

This linearized problem can be separated into three sub-problems using thin-wing theory from aerodynamics (see figure 3*b*). These are:

(i) the effect of angle of attack: for the flow around a zero-thickness un-cambered wing at an angle of attack of α, the boundary condition on the shells is

$$\frac{\partial \phi_1}{\partial z} = -U\alpha; \tag{14}$$

(ii) the effect of camber: for the flow around a zero-thickness cambered wing at zero angle of attack, the boundary condition on the shells is

$$\frac{\partial \phi_2}{\partial z} = U\frac{\partial h_c}{\partial x}; \tag{15}$$

(iii) the effect of thickness: for the flow around a symmetric wing with non-zero thickness at zero angle of attack, the boundary condition on the shells is

$$\frac{\partial \phi_3(x, y, \pm 0)}{\partial z} = \pm\left[U\frac{\partial h_{ts}}{\partial x} - U\beta(t) + (S_L - x)\frac{\mathrm{d}\beta(t)}{\mathrm{d}t}\right]. \tag{16}$$

ϕ_1, ϕ_2 and ϕ_3 are the perturbation potentials due to the angle of attack, camber, and thickness effect, respectively, and all satisfy the Laplace equation and the infinity condition; ϕ_1 and ϕ_2 also need to satisfy the Kutta condition at the trailing edge. Each of them can be solved independently. The complete solution for the scallop configuration, i.e. a thin cambered wing with variable thickness is

$$\phi(x, y, z, t) = \phi_1(x, y, z) + \phi_2(x, y, z) + \phi_3(x, y, z, t). \tag{17}$$

The linearized pressure coefficient derived from the unsteady Bernoulli equation using the small-disturbance approximation is

$$C_p(x, z, t) = \frac{p - p_\infty}{\frac{1}{2}\rho U^2} = -2\left(\frac{1}{U^2}\frac{\partial \phi}{\partial t} + \frac{1}{U}\frac{\partial \phi}{\partial x}\right). \tag{18}$$

ϕ_1 and ϕ_2 form the asymmetric steady lifting surface problem describing a flow around an infinitely thin cambered plate at an angle of attack. This gives a non-zero difference between the fluid pressures on the upper and lower shells and produces a net lift force and induced drag. The steady lifting-surface problem has been extensively studied for many aeronautical configurations (Katz & Plotkin 1991). According to thin-wing theory, there is a linear relationship between the lift and the angle of attack for thin wings in a flow at small angle of attack. Since scallops are much heavier than sea water, this conventional hydrodynamic lift plus the vertical component of the jet force is used to prevent sinking. We have applied the three-dimensional vortex ring panel method (Cheng, Zhuang & Tong 1991) to calculate the lift and induced-drag coefficients for the scallop configuration. We have shown that scallops have a small aspect ratio, and lack the best planform shape (Cheng & DeMont 1996), so that scallops have not evolved a shape that optimizes hydrodynamic properties in relation to the lift and drag forces. A hydrodynamic model for unsteady jet propulsion has been developed, in which the propulsion performance is characterized by three non-dimensional parameters: the storage-discharge volume ratio, reduced clapping frequency and reduced discharge frequency. Pulsed jet propulsion is designed to achieve high thrust at the expense of efficiency. The Froude efficiency (from about 0.3 to 0.5) is not necessarily as low as previously widely considered. The swimming mechanics describing the balance among the lift, jet thrust, gravity and drag on a swimming scallop have been evaluated to illustrate the swimming strategies and performance in relation to the ontogeny, external morphology and physiological parameters of the animal. These are given elsewhere (Cheng & DeMont 1996).

The thickness effect (ϕ_3) results in a velocity and pressure field symmetric about the commissural plane (x, y plane), and so does not produce net lift. It does not affect the momentum balance of the moving animal as a whole and is independent of the swimming mechanics mentioned above. However, the change in thickness with time during swimming is the result of the shell clapping powered by the adductor muscle contraction. This provides a time-dependent fluid force on each shell and in the same direction as the muscle force. The effects of angle of attack and camber produce a constant force which does not change with the shell opening and closing driven by the muscle contraction, and accounts for the buoyant weight. Thus it is only necessary to include the external fluid reaction due to the unsteady thickness effect in a model of the locomotor dynamics, and so it can be treated separately.

The unsteady symmetric flow is induced solely by the volume change of the scallop configuration, and will be solved here. The general solution of the potential flow problem can be obtained by superimposing elementary solutions of the Laplace

equation. The thickness effect can be modelled with a source singularity distribution (Cheng, Zhuang & Tong 1992). The source elementary solutions can be distributed on the $z = 0$ plane for the linearized problem (Katz & Plotkin 1991).

The scallop planform is close to a circle and for *Placopecten* (Dadswell & Weihs 1990) its aspect ratio ranges from 1.1 to 1.4 during growth. The three-dimensional effect of the thickness problem should be much smaller than that of the lifting problem, because the tip vortex produced with an angle of attack should be absent or weak in the symmetric flow. On most parts of the shell surface the spanwise (anterior-posterior) component (v) of the perturbation velocity should be much smaller than the chordwise (ventral-dorsal) component (u) and not larger than the third component (w) in the z-direction. Notice that the thickness is smaller than the shell width, and we have

$$\left|\frac{\partial v}{\partial y}\right| \ll \left|\frac{\partial u}{\partial x}\right|, \left|\frac{\partial w}{\partial z}\right|. \tag{19}$$

Thus at any spanwise station the three-dimensional Laplace equation can be approximated by a two-dimensional equation for the flow around the local symmetric airfoil. Since a two-dimensional analytical solution for the above thickness problem can be derived as given in the following Section, it is worthwhile to consider a quasi-two-dimensional case of the problem. The total hydrodynamic force on the three-dimensional symmetric body will be obtained as an integral of the forces on a set of unequal, quasi-two-dimensional longitudinal strips. The two-dimensional solutions basically set the upper limit of the three-dimensional solutions, i.e. the real perturbation velocity and hydrodynamic force of the three-dimensional flow may be lower than those of the quasi-two-dimensional flow.

3. Solution of two-dimensional flow

For a local longitudinal strip at any spanwise station, a two-dimensional flow around a symmetric airfoil with the leading edge at $x = x_L(y)$ and trailing edge at $x = x_T(y)$ is considered (figure 4). The chord length is $S_y = x_T(y) - x_L(y)$. In this section all quantities will be normalized by using swimming speed U and the local chord S_y as reference velocity and reference length, respectively. The potential and velocity fields are obtained by solving the two-dimensional Laplace equation and the boundary conditions (7) and (16) with y as a parameter. The airfoil thickness effect is modelled by a continuous distribution of the two-dimensional source singularities distributed along the commissural axis. The perturbation potential at any point (x, z) is then

$$\phi(x, z, t) = \frac{1}{2\pi}\int_0^1 \sigma(x_0, t) \ln\left[(x - x_0)^2 + z^2\right]^{\frac{1}{2}} \mathrm{d}x_0, \tag{20}$$

where $\sigma(x, t)$ is the strength function of the source singularity per unit length. (The subscript 3 of the potential due to the thickness effect (16) is omitted hereafter.) The two velocity components are

$$u(x, z, t) = \frac{\partial \phi}{\partial x} = \frac{1}{2\pi}\int_0^1 \sigma(x_0, t) \frac{(x - x_0)}{(x - x_0)^2 + z^2} \mathrm{d}x_0, \tag{21}$$

$$w(x, z, t) = \frac{\partial \phi}{\partial z} = \frac{1}{2\pi}\int_0^1 \sigma(x_0, t) \frac{z}{(x - x_0)^2 + z^2} \mathrm{d}x_0. \tag{22}$$

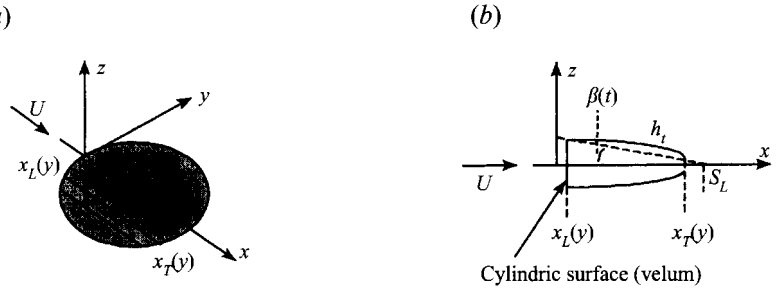

FIGURE 4. (*a*) Coordinate system of the thickness problem for a swimming scallop; the quasi-two-dimensional approximation is made for an arbitrary longitudinal strip. (*b*) Side view of the strip.

We can see from (20) to (22) that the potential (ϕ) and the x-component of the velocity (u) are symmetric, and the z-component (w) is antisymmetric with respect to the (x, y)-plane. Therefore the pressure distribution (18) due to the thickness effect is the same for the top and bottom surface, and no lift is produced. The velocity component in the z-direction at $z = 0$ can be evaluated as (Katz & Plotkin 1991)

$$w(x, \pm 0, t) \pm \tfrac{1}{2}\sigma(x, t). \tag{23}$$

Substituting (23) into the boundary condition (16) results in

$$\sigma(x,t) = \sigma_s(x) + \sigma_u(x,t), \quad \sigma_s(x) = 2\frac{\partial h_{ts}(x)}{\partial x}, \quad \sigma_u(x,t) = 2\left[-\beta(t) + (S_{Ly} - x)\frac{\mathrm{d}\beta(t)}{\mathrm{d}t}\right], \tag{24}$$

where σ_s and σ_u are the steady and unsteady parts of the source strength, respectively, and $S_{Ly} = S_L/S_y$. The solution of the thickness problem is obtained by substituting (24) into (20)–(22). Notice that the integrals in (20)–(22) are singular when $z = 0$, thus the Cauchy principal values should be taken. After integrations we have the potential along the x-axis as

$$\left.\begin{aligned}
\phi(x,0,t) &= \phi_s(x) + \phi_1(x)\,\beta(t) + \phi_2(x)\frac{\mathrm{d}\beta(t)}{\mathrm{d}t}, \\
\phi_s(x,z) &= \frac{1}{\pi}\int_0^1 \frac{\partial h_{ts}(x_0)}{\partial x}\ln\left[(x-x_0)^2 + z^2\right]^{1/2}\mathrm{d}x_0, \\
\phi_1(x) &= \frac{1}{\pi}\left[1 - x\ln x - (1-x)\ln(1-x)\right], \\
\phi_2(x) &= -\frac{S_{Ly}}{U}\phi_1(x) - \frac{1}{\pi}\left[-\frac{1}{4} - \frac{x}{2} + \frac{x^2}{2}\ln x + \frac{1}{2}(1-x^2)\ln(1-x)\right].
\end{aligned}\right\} \tag{25}$$

Substituting (25) into (18) yields the pressure on each shell evaluated on the $z = 0$ plane as

$$C_p(x,0,t) = C_{ps}(x) + C_{p1}(x)\,\beta(t) + C_{p2}(x)\frac{\mathrm{d}\beta(t)}{\mathrm{d}t} + C_{p3}(x)\frac{\mathrm{d}^2\beta(t)}{\mathrm{d}t^2}. \tag{26}$$

We are interested in the total force, and particularly the moment about the hinge, due to the outer fluid reaction on each shell. The forces and moments on the upper and lower shells have the same magnitude but act in opposite directions. We will choose the

force and moment on the upper shell, the negative of these quantities will represent those on the lower shell. The coefficient of the force (positive in positive z-direction) on the upper shell can be derived as

$$\left.\begin{aligned} C_F &= \frac{F}{S_y q} = -\int_0^1 C_p(x,0,t)\,\mathrm{d}x = C_{Fs} + C_{F1}\beta(t) + C_{F2}\frac{\mathrm{d}\beta(t)}{\mathrm{d}t} + C_{F3}\frac{\mathrm{d}^2\beta(t)}{\mathrm{d}t^2} \\ C_{Fs} &= 2\int_0^1 \frac{\partial \phi_s}{\partial x}\mathrm{d}x, \quad C_{F1} = 0, \quad C_{F2} = \frac{4}{\pi}, \quad C_{F3} = -\frac{3}{2\pi}S_{Ly}. \end{aligned}\right\} \tag{27}$$

The coefficient of the moment about the hinge $x = S_{Ly}$, $z = 0$ (positive in the clockwise direction) is

$$\left.\begin{aligned} C_M &= \frac{M}{S_y^2 q} = -\int_0^1 (S_{Ly} - x)\, C_p(x,0,t)\,\mathrm{d}x = C_{Ms} + C_{M1}\beta(t) + C_{M2}\frac{\mathrm{d}\beta(t)}{\mathrm{d}t} \\ &\quad + C_{M3}\frac{\mathrm{d}^2\beta(t)}{\mathrm{d}t^2}, \\ C_{Ms} &= -2\int_0^1 (S_{Ly} - x)\frac{\partial \phi_s}{\partial x}\mathrm{d}x, \quad C_{M1} = \frac{1}{\pi}, \quad C_{M2} = \frac{3}{2\pi}S_{Ly}, \\ C_{M3} &= -\frac{1}{4\pi}(3S_{Ly}^2 + \tfrac{1}{2}). \end{aligned}\right\} \tag{28}$$

4. Hydrodynamic loads

The solution obtained in §3 is composed of two parts: a steady part associated with the steady thickness distribution of the scallop when the shells are closed, and an unsteady part associated with the expansion and contraction of the boundary. The steady part can be calculated from measurements of the thickness distribution for the specific species. The unsteady part of the fluid force was found to be independent of the configuration of a specific species. In fact, the unsteady part is a quasi-two-dimensional solution of an object with an isosceles triangle section with base facing and perpendicular to the oncoming flow (figure 4*b*). The upper and lower straight side lines of the triangle pitch around the hinge and do not pass through the mean surface $z = 0$.

The force and moment per unit span can be rewritten in dimensional form as

$$F(y) = F_s + F_2 + F_3 = F_s(y) + \frac{2}{\pi}\rho U S_y^2 \frac{\mathrm{d}\beta}{\mathrm{d}t} - \frac{3}{4\pi}\rho S_L S_y^3 \frac{\mathrm{d}^2\beta}{\mathrm{d}t^2}, \tag{29}$$

$$M(y) = M_s + M_1 + M_2 + M_3 = M_s(y) + \frac{1}{2\pi}\rho U^2 S_y^2 \beta + \frac{3}{4\pi}\rho U S_L S_y^2 \frac{\mathrm{d}\beta}{\mathrm{d}t} - \frac{S_y^2}{16\pi}\rho(6S_L^2 + S_y^2)\frac{\mathrm{d}^2\beta}{\mathrm{d}t^2}. \tag{30}$$

Notice that the above force and moment act only on part of the entire wetted surface of the animal, namely on the outer surface of one shell. This is different than the usual cases in which the fluid-dynamic forces are derived for the whole immersed body.

We will focus on the moment about the hinge, since it will be used directly in our dynamic model of the swimming system. If we take the scallop commissural planform

as a circular shape, integrating the moment (30) over all unequal longitudinal strips gives the total moment for each shell as

$$M = 2\int_0^{S_L/2} M(y)\,\mathrm{d}y = M_s + k_f\beta(t) + c_f\frac{\mathrm{d}\beta(t)}{\mathrm{d}t} - I_f\frac{\mathrm{d}^2\beta(t)}{\mathrm{d}t^2}, \tag{31}$$

where

$$M_s = \rho U^2\int_0^{S_L/2} C_{Ms}\,\mathrm{d}y, \tag{32}$$

$$k_f = \frac{1}{3\pi}\rho U^2 S_L^3, \quad c_f = \frac{1}{2\pi}\rho U S_L^4, \quad I_f = \frac{17}{60\pi}\rho S_L^5. \tag{33}$$

The unsteady moment due to the symmetric thickness effect is represented by three terms which are proportional to the deformation itself, and the first and second derivatives of the deformation, respectively. Each term in (31) will be analysed in the following subsections.

4.1. *Added mass*

The last term in (31) results from the angular acceleration of the shell and I_f is equivalent to the added moment of inertia (or added mass in a rectilinear motion). For *Placopecten magellanicus* the ratio of shell weight (m_v) to shell area (A_v) in relation to shell length was measured by Dadswell & Weihs (1990). At $S_L = 0.055$ m, for example, for one shell the value of the ratio of shell weight to shell area is

$$m_v/A_v = 1.9\ \mathrm{kg\ m^{-2}}.$$

Suppose that the mass of shell is uniformly distributed over the projected circle; the moment of inertia for one shell is then

$$I_v = \frac{5\pi}{64}S_L^4\left(\frac{m_v}{A_v}\right) = 4.26\times10^{-6}\ \mathrm{kg\ m^2}$$

and the added moment of inertia as calculated from (33) is

$$I_a = 46.32\times10^{-6}\ \mathrm{kg\ m^2}.$$

The added moment of inertia can be ten times larger than the moment of inertia of the shell itself. Thus for scallop swimming, the dominant inertia in the dynamic system is the added mass. The fluid acceleration reaction will significantly influence the shell oscillation.

4.2. *Flow-induced pseudo-elasticity*

The second term on the right hand side of (31) is the unsteady moment proportional to the gape angle $\beta(t)$. This displacement force has a form similar to a linear elastic force and also increases with the displacement. The elastic force of the hinge ligaments resists closing and increases as the gape angle decreases, but this fluid force decreases as the gape angle decreases. We call this term the flow-induced pseudo-elasticity force. It provides an opening force over the whole cycle. During the opening phase of the cycle this force assists shell opening, but during the closing phase it acts to oppose the effort of the muscle contraction. From (29) to (30) the flow pseudo-elasticity gives zero force, but a couple. The rotational pseudo-stiffness k_f depends on the fluid density, swimming speed and body size.

The pseudo-stiffness can be estimated and compared to the measured stiffness of hinge ligaments. Vogel (1985) measured the rotational stiffness of the hinge ligament

Species	Size: S_L (m)	Speed: U (m s^{-1})	Source
Chlamys opercularis	0.065–0.075	0.30	Moore & Trueman (1971)
Chlamys islandica	0.010–0.020	0.15	Gruffydd (1976)
Chlamys islandica	0.065–0.075	> 0.35	Gruffydd (1976)
Amusium pleuronectes	0.065–0.10	0.37–0.45	Morton (1980)
Placopecten magellanicus	0.030–0.10	0.30–0.60	Dadswell & Weihs (1990)

TABLE 1. Swimming speeds of scallops

for a 0.066 m long *Pecten irradians*. From his figure 2 the rotational stiffness (k) was estimated to be about 0.083 N m. The swimming speed is needed to evaluate the pseudo-stiffness, but was not given in his paper. The measured and estimated swimming speeds for other species are listed in table 1. Higher swimming speeds were reported for some species (e.g. 0.73 m s^{-1} in Morton 1980). We take a value of 0.5 m s^{-1} as an example in our calculation, which is the same as that chosen by Vogel (1985). Then from (33)

$$k_f = 0.0078 \text{ N m}, \quad \text{or} \quad k_f/k = 9.4\%.$$

DeMont (1990) also measured the stiffness of the hinge for *Pecten maximus*. For a 0.0854 m long individual the stiffness was estimated to be 0.29 N m. Its pseudo-stiffness at the swimming speed of 0.5 m s^{-1} can be calculated as

$$k_f = 0.017 \text{ N m}, \quad \text{or} \quad k_f/k = 5.9\%.$$

Thus, for the two examples above, during shell oscillations the pseudo-elasticity generated by the outer flow may provide forces of about 9.4% and 5.9% of the hinge elastic forces. Notice that with increasing gape angle the pseudo-elastic force increases, but the hinge elastic force decreases. Therefore the flow-induced pseudo-elasticity makes larger instantaneous contributions at larger gape angles. Furthermore the pseudo-elasticity is proportional to the square of the speed and the cube of the size, so that for larger and/or faster swimming animals the pseudo-elasticity may be further enhanced.

4.3. *Flow-induced pseudo-viscosity*

We now look at the term in (31) proportional to the angular velocity. This force has a form similar to that of a linear dashpot. Again the function of the fluid force is different than the damping force and it acts in the same direction as the velocity of shell. For convenience we call it the flow-induced pseudo-viscosity. Since it acts in the direction of the shell velocity, it will assist the hinge ligaments in opening the shell and the adductor muscle in closing the shell.

Bowie *et al.* (1993) measured the damping in the hinge of *Placopecten magellanicus*. The damping is temperature-dependent, and increases as temperature decreases. From their figure 2, at 10 °C the resilience (R) of the intact hinge was about 79%. The resilience is defined as

$$\ln(100/R) = 2\delta, \tag{34}$$

where δ is the natural logarithmic decrement. If the damping effect could be modelled by a viscous dashpot which is assumed to be parallel to the elastic element of the hinge, then the damping factor is (Thomson 1988)

$$\zeta = \frac{c}{c_c} = \left(\frac{\delta^2}{4\pi^2 + \delta^2}\right)^{1/2}, \tag{35}$$

Shell height, S_L (m)	Hinge viscosity, c (kg m^2 s^{-1})	Pseudo-viscosity, c_f (kg m^2 s^{-1})
0.0875	0.0041	0.0048
0.0895	0.0056	0.0052
0.0908	0.0059	0.0055
0.101	0.0129	0.0085

TABLE 2. Viscous coefficients for the flow-induced pseudo-viscosity and the hinge damping of *Placopecten magellanicus* at 10 °C

where c is the viscous coefficient of the hinge, and c_c is the critical viscous coefficient. The damped vibration frequency (f_d) was taken as 3 Hz in their experiments. Thus the viscous coefficient of the hinge at 10 °C is

$$c = \frac{4\pi f_d \zeta}{(1-\zeta^2)^{1/2}} I = 14.54\, I, \tag{36}$$

where I is the moment of inertia about the hinge for the shell and the weight added to the top shell on which the free damped oscillation tests were performed. The values of c for four samples are listed in table 2.

The pseudo-viscosity coefficients can be calculated by (33) and values for the same samples at $U = 0.5$ m s^{-1} are also listed in table 2. The pseudo-viscosity coefficients are very close to the hinge viscous coefficients at 10 °C. The flow-induced viscosity almost compensates for the effect of the hinge damping. The energy lost in the hinge damping is fed back from the surrounding flow. The hinge–shell–outer-fluid system of a swimming scallop may work with very little damping.

4.4. *Steady moment*

The steady part of the total moment depends on the specific airfoil shape, i.e. $h_{ts}(x, y)$ defined in (12), which is the average surface of the lower and upper shells. For different species and even different individuals the thickness distributions are different. The steady part M_s plus the pseudo-elasticity term $M_1 = k_f \beta$ are often called the quasi-steady contribution of the fluid reaction. They are the solutions for steady flow past an instantaneous configuration of the subject. For a section with an elliptical shape the steady pressure coefficient along the chord is (Katz & Plotkin 1991)

$$C_{ps} = -2(t_m/S_y), \tag{37}$$

where t_m is the maximum thickness (top-bottom height). This pressure coefficient is constant along the chord. However, the cross-sectional shape of the scallops is generally not close to an ellipse. For other cross-sectional shapes pressure distributions can be similarly obtained by integrating (25).

A thickness surface with a parabolic chordwise (ventral–dorsal) and linear spanwise (anterior–posterior) distribution, can better approximate a scallop section. At an arbitrary point (x, y), we have

$$\left.\begin{aligned} h_{ts}(x,y) &= 4t(y)\frac{x-x_L(y)}{S_y(y)}\left(1-\frac{x-x_L(y)}{S_y(y)}\right), \quad x_L(y) \leqslant x \leqslant x_T(y), \\ t(y) &= \tfrac{1}{2}t_m(1-|2y/S_L|), \quad -\tfrac{1}{2}S_L \leqslant y \leqslant \tfrac{1}{2}S_L, \end{aligned}\right\} \tag{38}$$

where t_m is the maximum thickness at the middle of the shell, and $S_y(y)$ the length

between the leading (ventral) edge and trailing (dorsal) edge at a spanwise location. Substituting (38) into (25) and (28) we can obtain the steady moment on one shell about the hinge as

$$M_s = \frac{1}{2\pi}\rho U^2 t_m S_L^2. \tag{39}$$

If we take $t_m/S_L = 0.2$ and $\beta_m = 5°$, which are representative value for most swimming scallops, the ratio of the steady moment to the pseudo-elastic moment is

$$\frac{M_s}{M_1} = \frac{3}{2}\frac{(t_m/S_L)}{\beta_m} = 3.4. \tag{40}$$

The steady part of the total moment is higher than the part proportional to the angular displacement.

5. Discussion

Generally, the small-disturbance solution can give accurate predictions for most parts of the flow region. However, the solution may not be very good in some localized regions, such as near the front and rear stagnation points. If the thickness decreases, the stagnation region becomes smaller and the solution will move closer to the exact solution. Since the stagnation regions are small compared to the remaining part of the chord length, the total force and moment on the shells can be predicted quite well by the small-disturbance theory.

Vogel's measurements (1985) are the only available fluid force data on scallops that can be used to make a comparison with the present theory. For a 0.066 m long *Pecten irradians* swimming at 0.5 m s^{-1}, Vogel measured the pressure distribution on the outer surface of the shells when they were closed and opened at a gape angle of 13.3°. For the open shells, a piece of brass plate on which the flow pressure was measured was fitted on the gape. For the closed shells, the moment about the hinge tending to open the shells, averaged from the values of two shells, was calculated to be 0.001 80 N m. This moment should correspond to the steady moment M_s in (31). Assuming a thickness ratio $t_m/S_L = 0.2$, the same swimming speed $U = 0.5$ m s^{-1} and a shell height $S_L = 0.066$ m, the steady moment from the present theory (39) is $M_s = 0.002\,30$ N m. The theoretical value is higher than the measured value. The theoretical value is calculated for a thickness surface with a parabolic chordwise arc and the maximum thickness located at the centre as given by (38). Most scallops, including *Pecten irradians*, have a more gentle increase in the thickness on the ventral surface. The maximum thickness is located behind the centre and there is a more rapid decrease on the dorsal surface. Such a thickness distribution will give a lower pressure on the ventral part of the shell surface than the parabolic thickness distribution. This will reduce the moment about the hinge, so that the theoretical prediction will be closer to the measured value.

The difference between the measured moment for the closed and gaped shells should be equivalent to the pseudo-elasticity term in (31). When the shells were opened, the moment due to pressure on each shell was 0.002 02 N m, and the moment due to the pressure at the gape (on the brass plate) was 0.002 60 N m. The two values were added to give an overall moment tending to open the shell of value 0.003 28 N m. The moment for the closed shells was 0.001 80 N m. The difference between the moments of the gaped and closed valves is then 0.001 48 N m, and if the pressure on the gape is not

taken into the estimation the difference in the moments is 0.000 22 N m. The theoretical moment (31) for the same gape angle is 0.000 90 N m, which is between the measured value with and without the gape pressure contribution.

The flow around the gape has two components: the flow turns up and down to pass around the ventral edge (two corners of the triangle profile), and the flow is sucked into the mantle cavity during the refilling part of the cycle. Vogel did not consider the sucking flow itself in his experiments, but supposed that during the whole cycle all fluid around the ventral region is sucked into the cavity and pushes the shells open. Such treatment is not adequate. First, the flow component of sucking into the mantle cavity only occupies part of the cycle, i.e. in the valve opening phase. Secondly, the fluid force acting on the internal surface of the shell due to flow into the mantle cavity is not equivalent to that resulting from the flow around the stagnation region at the ventral gape as measured in the experiments. Furthermore, the outer flow component exists during the whole cycle. The gape pressure in Vogel's measurements will partly contribute to the formation of the rapid outer flow leaving the stagnation point and moving around the upper and lower corners at the ventral edge. This contributes to the total force of the outer flow obtained in the present work. In other words, the opening moment due to the outer flow, based on Vogel's measurements, should be between the two values above, in agreement with our theoretical value.

A time-independent negative pressure exists on each shell at any instant during swimming. This results in a force and moment constantly acting to open the valves during the whole clapping cycle. The moment for a specific species can be calculated by (25) and (28) using the measured thickness distribution. However, the steady part does not participate in the dynamic process of the system, and should be balanced by the material stiffness associated with the muscle and outer hinge ligaments connecting the two shells. Thus it will not be included in the dynamic model of the locomotor system, although the steady part may be even higher than M_1.

The effect of fluid acceleration on aquatic locomotion has been emphasized (Daniel 1984). The present analytical solutions precisely show the structure of the unsteady fluid force due to the thickness effect. The force has three terms, which are proportional to the deformation itself, and the first and second derivatives of the deformation. The flow-induced pseudo-elasticity and -viscosity are related to the swimming speed, but the added mass is not. The added-mass force always exists as long as the scallop is clapping the shells. The pseudo-elasticity and -viscosity will be very small at low swimming speeds. It has been shown that the unsteady forces (lateral force and thrust) on a swimming fish are not determined only by the lateral acceleration of the body, but are greatly influenced by the vortex wake carrying information on the undulation history of the body and tail (Wu 1971; Lighthill 1975; Blickhan & Cheng 1994). The present unsteady side hydrodynamic forces on swimming scallops, although without the wake contribution, are also not simply proportional to the acceleration of the shell. In general, the reaction of the fluid on a swimming animal performing unsteady motion may depend on the whole history of the body motion. The derivatives of motion of all orders with respect to time may influence the fluid force.

Recent studies (DeMont & Gosline 1988; Bowtell & Williams 1994; Cheng & Blickhan 1994) have shown that the dynamics and energetics of aquatic locomotion should combine all mechanical elements associated with the swimming animal. The mechanical energy generated by the muscles not only contributes to the propulsive hydrodynamic work, but also powers the reciprocal movement of the locomotor apparatus. The unsteady side fluid force which acts on the external surface of the animal and directly interacts with the muscle contraction has generally been ignored in

studies of aquatic jet-propelled locomotion. This fluid reaction can be one of the important dynamic elements in the locomotor system, and will be included in our dynamic studies. Generally, a phase delay exists between the movement and the unsteady force, and may make the system optimize energy savings. The *in vivo* working behaviour, the mechanical design of the relevant tissues and the neural control of the locomotion will be influenced by this fluid reaction.

The pallial curtain (velum) between the parted shells regulates the flow through the ventral mantle margin and flow in the mantle cavity during the shells opening. The inward and outward flows will generate forces in the swimming direction, but their influence on the vertical force on the shell is considered small. Since the present work is the first dealing with the side hydrodynamic forces in scallop swimming, indeed in all jet-propelled locomotion, we have used a simplified model to get meaningful results and to evaluate the possible importance of this fluid reaction. The real influence of the inward and outward flow on the outer flow over the shell has not been quantitatively evaluated in this analytical work. A potential flow model including the inward and outward flows has been suggested in §2.1. A boundary element method for potential flow past bodies with arbitrary three-dimensional shapes (Cheng *et al.* 1992) may be suitable to model this complex phenomenon.

This research was supported by grants from NSERC (Operating) and ACOA (Interim Funding Research Project) to M.E.D. J.Y.C. was supported by an NSERC International Fellowship and St.F.X. We thank Dr E. Kenchington (DFO, Halifax) for supplying the scallops, Dr S. Vogel for reading an early version of the manuscript, and the anonymous referees for their comments.

REFERENCES

AHMADI, A. R. & WIDNALL, S. E. 1986 Energetics and optimum motion of oscillating lifting surfaces of finite span. *J. Fluid Mech.* **162**, 261–282.

ALEXANDER, R. MCN. 1977 Swimming. In *Mechanics and Energetics of Animal Locomotion* (ed. R. McN. Alexander & G. Goldspink), pp. 222–247. Chapman and Hall.

BELOTSERKOVSKII, S. M. 1977 Study of the unsteady aerodynamics of lifting surfaces using the computer. *Ann. Rev. Fluid Mech.* **9**, 469–494.

BLICKHAN, R. & CHENG, J.-Y. 1994 Energy storage by elastic mechanisms in the tail of large swimmers – a re-evaluation. *J. Theor. Biol.* **168**, 315–321.

BOWIE, M. A., LAYES, J. D. & DEMONT, M. E. 1993 Damping in the hinge of the scallop *Placopecten magellanicus*. *J. Exp. Biol.* **175**, 311–315.

BOWTELL, G. & WILLIAMS, T. L. 1994 Anguilliform body dynamics: a continuum model for the interaction between muscle activation and body curvature. *J. Math. Biol.* **32**, 83–91.

CHENG, J.-Y. & BLICKHAN, R. 1994 Bending moment distribution along swimming fish. *J. Theor. Biol.* **168**, 337–348.

CHENG, J.-Y., DAVISON, I. G. & DEMONT, M. E. 1996 Dynamics and energetics of scallop locomotion. *J. Exp. Biol.* (accepted).

CHENG, J.-Y. & DEMONT, M. E. 1996 Jet-propelled swimming in scallops: swimming mechanics an ontogenic scaling. *Can. J. Zool.* (submitted).

CHENG, J.-Y., ZHUANG, L.-X. & TONG, B.-G. 1991 Analysis of swimming three-dimensional waving plates. *J. Fluid Mech.* **232**, 341–355.

CHENG, J.-Y., ZHUANG, L.-X. & TONG, B.-G. 1992 The local linearization boundary element method with application to high subsonic flow past body. *Engng Anal. with Boundary Elements* **10**, 193–197.

DANIEL, T. L. 1984 Unsteady aspects of aquatic locomotion. *Am. Zool.* **24**, 121–134.

DADSWELL, M. J. & WEIHS, D. 1990 Size-related hydrodynamic characteristics of the giant scallop *Placopecten magellanicus* (Bivalvia: Pectinidae). *Can. J. Zool.* **68**, 778–785.

DeMont, M. E. 1990 Tuned oscillations in the swimming scallop *Pecten maximus*. *Can. J. Zool.* **68**, 786–791.

DeMont, M. E. 1992 Locomotion of soft bodied animals. In *Advances in Comparative and Environmental Physiology*, vol. 11 (ed. R. McN. Alexander), pp. 167–190. Springer.

DeMont, M. E. & Gosline, J. M. 1988 Mechanics of jet propulsion in the hydromedusan jellyfish *Polyorchis penicillatus* 2. Energetics of the jet cycle. *J. Exp. Biol.* **134**, 333–345.

Gould, S. J. 1971 Muscular mechanics and the ontogeny of swimming in scallops. *Paleontology (Lond.)* **14**, 61–94.

Gruffydd, L. D. 1976 Swimming in *Chlamys islandica* in relation to current speed and an investigation of hydrodynamic lift in this and other scallops. *Norw. J. Zool.* **24**, 365–378.

Hayami, I. 1991 Living and fossil scallop shells as airfoils: an experimental study. *Paleobiology* **17**(1), 1–18.

Katz, J. & Plotkin, A. 1991 *Low Speed Aerodynamics: From Wing Theory to Panel Method.* McGraw-Hill.

Lighthill, M. J. 1975 *Mathematical Biofluiddynamics*. SIAM.

McCrosky, W. J. 1982 Unsteady airfoils. *Ann. Rev. Fluid Mech.* **14**, 285–311.

Madin, L. P. 1990 Aspects of jet propulsion in salps. *Can. J. Zool.* **68**, 765–777.

Marsh, R. L., Olson, J. M. & Quzik, S. K. 1992 Mechanical performance of scallop adductor muscle during swimming. *Nature* **357**, 411–413.

Millward, A. & Whyte, M. A. 1992 The hydrodynamic characteristics of six scallops of the Super Family Pectinacea, Class Bivalvia. *J. Zool. (Lond.)* **227**, 547–566.

Moore, J. D. & Trueman, E. R. 1971 Swimming of the scallop, *Chlamys opercularis* (L.). *J. Exp. Mar. Biol. Ecol.* **6**, 179–185.

Morton, B. 1980 Swimming in *Amusium pleuronectes* (Bivalvia: Pectinidae). *J. Zool. (Lond.)* **190**, 375–404.

O'Dor, R. K. 1988 The force acting on swimming squid. *J. Exp. Biol.* **137**, 421–442.

Stanley, S. M. 1970 Relation of shell form to life habits in the Bivalvia (Mollusca). *Mem. geol. Soc. Am.* **125**, 1–296.

Thomson, W. T. 1988 *Theory of Vibration with Applications*. Prentice Hall.

Trueman, E. R. 1975 *The Locomotion of Soft-bodied Animals*. Edward Arnold.

Vogel, S. 1985 Flow-assisted shell reopening in swimming scallops. *Biol. Bull. (Woods Hole, Mass.)* **169**, 624–630.

Weihs, D. 1977 Periodic jet propulsion of aquatic creatures. *Fortschr. Zool.* **24**, 171–175.

Wu, T. Y. 1971 Hydrodynamics of swimming fishes and cetaceans. *Adv. Appl. Maths* **11**, 1–63.